

Article

A Study on Performance Evaluation of Biodiesel from Grape Seed Oil and Its Blends for Diesel Vehicles

Adebayo Fadairo ¹ and Weng Fai Ip ^{2,*}

¹ Department of Electromechanical Engineering, Faculty of Science and Technology, University of Macau, Macau 999078, China; afadairo@ouufe.edu.ng

² Department of Physics and Chemistry, Faculty of Science and Technology, University of Macau, Macau 999078, China

* Correspondence: andyip@um.edu.mo

Abstract: With incessant increases in fuel prices worldwide and concerns for environmental pollution, the need for alternative sources of energy is becoming urgent. In this study, the potential of grape seed oil for biodiesel as an alternative fuel was evaluated. Refined grape seed oil was bought in liquid form and then subjected to an alkali-catalyzed transesterification process for biodiesel production. The physicochemical properties of the resulting biodiesel—namely, viscosity, cetane number, and heating value—were investigated. The biodiesel was blended with a conventional diesel in various proportions and combusted in a four-cylinder, four-stroke compression ignition (diesel) engine under two loading conditions. Experimental results revealed that the blend ratio of B70 (70% GS biodiesel and 30% conventional diesel) gave the best overall engine performance in terms of maximum power, minimum emissions, and fuel consumption. Furthermore, a novel neural network technique called extreme learning machine was adopted to investigate the optimal blend ratio using the dataset obtained from the experimental results. The results also indicate that the best choice of biodiesel blend ratio is approximately B73.67 (73.67% GS biodiesel and 26.33% conventional diesel). The study shows that grape seed oil could serve as a reliable source of production of quality biodiesel fuels, which could be used as an alternative to conventional diesel fuels.



Citation: Fadairo, A.; Ip, W.F. A Study on Performance Evaluation of Biodiesel from Grape Seed Oil and Its Blends for Diesel Vehicles. *Vehicles* **2021**, *3*, 790–806. <https://doi.org/10.3390/vehicles3040047>

Academic Editor: Mohammed Chadli

Received: 26 August 2021

Accepted: 27 October 2021

Published: 23 November 2021

Publisher's Note: MDPI stays neutral with regard to jurisdictional claims in published maps and institutional affiliations.



Copyright: © 2021 by the authors. Licensee MDPI, Basel, Switzerland. This article is an open access article distributed under the terms and conditions of the Creative Commons Attribution (CC BY) license (<https://creativecommons.org/licenses/by/4.0/>).

1. Introduction

In the past century, the rapid development of industry, population growth, and the simultaneous improvement in people's living standards were significantly aided by the use of fossil fuels. Burning fossil fuels produces large amounts of carbon dioxide, which aggravates global warming [1]. In addition, as fossil fuels are limited resources, reducing fuel consumption and the development of green energy sources are important millennium development goals for sustainability [2]. From an Energy Information Administration (EIA) report on short-term energy outlook, it is projected that total world oil production in 2022 will be 101.81 million barrels per day [3]. As the global population remains on an upward trajectory, global consumption is unlikely to slow down in the immediate future. Therefore, there are great incentives for exploring alternative energy sources.

The production of biofuel is economically significant, as it does not require the phasing out of existing engines immediately, allowing us to buy time for investigating and developing other alternative, sustainable energy sources. Biofuel has been widely considered as one of the renewable energies that can be used on a daily basis [4]. Two common types of biofuel are produced—namely, bioethanol and biodiesel. Biodiesel is a renewable fuel made from biomass sources including both vegetable oils and animal fats. Biodiesel is suitable for diesel engines, whereas bioethanol is suitable for gasoline engines. The shift from conventional diesel to biodiesel as a fuel in CI engines poses less threat to the environment, since biodiesel is biodegradable, nontoxic, and renewable. The combustion

of biodiesel in CI engines releases remarkably fewer harmful substances in the emissions when compared to conventional diesel, which poses a major concern [5].

The search for sustainable sources of biofuels has prompted investigators to test a wide range of crops—from sugarcane, to rapeseed, to canola oil [6–8]. One important factor with a great impact on the plant-based crops is that their utilization for biodiesel production will not threaten the existing reliance on their use as a food source, which could cause turbulence in commodity pricing [9,10]. In 2005, the overall production of grapes—mainly to be further processed to wine production—was over 67 million tons per year, of which the grape seed carries little to no commercial value and is dumped. Grape seeds typically contain around 20% lipids, which is significantly high compared to other potential sources of biodiesel [11]. This provides the impetus for grape seed oil as feedstock for biodiesel production. In the past few years, many studies have been conducted on biodiesel production [12,13]. There are, however, only a few reports about the engine performance and emissions using biodiesel in a CI (diesel)-engine-powered vehicle. The power output and exhaust emissions of a single cylinder with a four-stroke diesel engine are commonly used to examine biodiesels and their blends [14–17]. Owing to inefficient combustion of conventional diesel, harmful substances such as carbon monoxide (CO), nitrogen oxides (NO_x), and hydrocarbons (HC) are often generated and released through exhausts, with an adverse effect on the environment and human health. In addition, conventional diesel is a fossil fuel, and is considered non-renewable. Consequently, advocates for phasing out fossil fuels gradually gain support as the production of alternative energy sources gains traction. Without any major modification of an engine, biodiesel is a popular alternative energy source for diesel fuels, and has the potential to reduce exhaust emissions. In practice, biodiesels are mixed with conventional diesel for performance enhancement, which is subject to optimizing the blend ratio. According to Di [18], an increase in the amount of biodiesel in diesel leads to a reduction in CO and particulate matter emissions, while fuel economy and NO_x emissions increase. The composition of the feedstocks of biodiesel typically consists of a combination of the following compounds: simple alkyl esters of fatty acids produced from vegetable oils and animal fats, consisting of long-chain alkyl (methyl, ethyl, or propyl) esters. Due to their high ignition points and the viscosity of lipids and fats, they are not suitable to be used directly as a liquid fuel, hence the need for a process to convert lipids or fats into esters. Biodiesel is generally used as a blend with conventional diesel [19]. In the past few years, many studies have been devoted to the study of biodiesel production—principally from the oils and fats of plants such as canola, jatropha, palm oil, soybean, and sunflower [8,19–23]. The novelty of this study lies in the use of a four-cylinder, four-stroke compression ignition (CI) engine for the investigation of the performance of the resultant biodiesel and its blends. The impetus for the study was from the research conducted by Silvia Mironesa et al. in 2010 on the physicochemical properties, structural characteristics, and oil content of grape seeds, which proposed grape seed oil as a potential feedstock for the production of biodiesel as an alternative source of fuel for powering diesel engines [24]. No existing studies have considered the performance of biodiesel made from grape seed oil (GSO), and its blends with conventional diesel, in a CI (diesel)-engine-powered vehicle. Consequently, our intention is to fill the gap in the knowledge and provide a platform for the continuous investigation of the use of biofuels in engines. However, the technology for utilizing biodiesel alone in CI engines is not yet available, so biodiesel is blended with conventional diesel for use. It is therefore imperative to determine the optimal blend ratio that gives the best performance with respect to emissions, fuel economy, and power output. Furthermore, our study adopts an artificial learning method—extreme learning machine (ELM)—for the optimization of biodiesel blends. This method considers a new learning scheme for a single-hidden-layer feedforward neural network (SLFN), as proposed in [25]. ELM can randomly initialize the input weight and bias to get the corresponding output weight for an SLFN.

This paper is arranged in the following order: the production of FAME from grape seed oil; test in a CI engine (diesel)-powered vehicle; and optimization of blending ratio

using experimental results, followed by the determination of overall best performance and conclusion.

2. Materials and Methods

The material used in this study was grape seed oil. Commercial grade grape seed oil was bought in liquid form. The grape seed oil was then processed via transesterification to produce biodiesel.

2.1. Production of Biodiesel

Studies have shown that reaction time and temperature are the main factors affecting the yield of ester [25]. In addition, the use of catalysts, such as alkaline metal hydroxides (KOH and $(\text{CH}_3\text{NaO})_2$), speeds up the conversion [26]. Transesterification is a well-known and cheap standard process that turns lipids or fats into esters. The procedure for transesterification was diligently followed, as described in [27]. Briefly, the procedures were as follows: Grape seed oil was reacted with methanol using sodium hydroxide as a catalyst stoichiometrically, at a methanol-to-oil molar ratio of 9. Heating was maintained at 55°C , and the mixture was stirred at 120 rpm for 2 h using a thermostat hot plate. Upon the completion of the reaction, the products separated into two layers: an upper layer (ester) and a lower layer (glycerol and impurities). The filtered upper layer containing the ester was then transferred into a rotary evaporator with the water bath maintained at 75°C for the removal of residual methanol. Next, the obtained biodiesel was washed thoroughly using warm, distilled water until it was free of base. The washed biodiesel formed at the upper layer was then stored for further analysis. An AGILENT GC 7890 gas chromatograph and 5975 C mass spectrometer with column model Agilent 19091S-433 ($30\text{ m} \times 250\text{ }\mu\text{m} \times 1\text{ }\mu\text{m}$) and helium carrier gas were used to assess the fatty acid composition of the biodiesel. The chromatograph obtained from GC-MS is as shown in Figure 1 while Table 1 presents the average percentage composition of the fatty acid fragment in GS FAME.

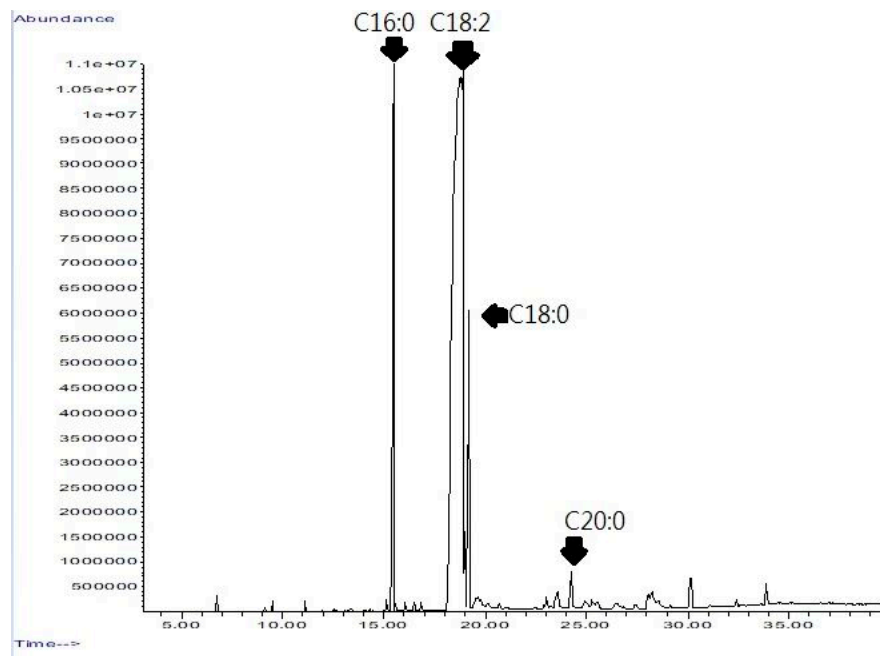


Figure 1. Chromatograph of grape seed FAME.

Table 1. Average % composition of the fatty acid fragment in GS FAME.

Fatty Acid Fragment of Methyl Ester	GS FAME
Palmitic acid (C16:0)	13.39
Stearic acid (C18:0)	5.60
Linoleic acid (C18:2)	80.17
Arachidic acid (C20:0)	0.84

2.2. Blend Preparation

Two types of fuel in pure and blended forms were tested on a diesel vehicle engine—namely, conventional diesel (DI) and grape seed (GS) FAME. Table 2 shows the blend proportions:

Table 2. Blend proportions.

Blend	Blend Ratio
I	B0 (100% DI)
II	B30 (30% GS + 70% DI)
III	B50 (50% GS + 50% DI)
IV	B70 (70% GS + 30% DI)
V	B100 (100% GS)

The specifications of the vehicle used for the experimentation is as presented in Table 3 below:

Table 3. Specifications of the test vehicle.

Model	Daihatsu Rocky 2.8 Diesel Hardtop
Engine type	Naturally aspirated, in-line 4-cylinder
Fuel system	Diesel indirect injection
Maximum power	54 kW @ 3600 rpm
Maximum torque	170 Nm @ 2200 rpm
Bore × stroke	92.0 mm × 104.0 mm
Engine size (displacement)	2765 cc
Compression ratio	21.5:1

A specific modification was made to the test vehicle prior to the commencement of testing: the instalment of the fuel tank outside of the engine compartment, for proper monitoring of fuel consumption and quick fuel replenishment. The fuel tank capacity was ~1 L, and the final setup is shown in Figure 2. The schematic representation of the experimental set up is shown in Figure 3.

2.3. Smoke Test

A Wager Model 6500 Smoke (Opacity) meter was set up at the tailpipe of the diesel vehicle. The smoke meter displays the smoke opacity in Hartridge smoke units (HSUs) under the free acceleration test. The measurement of smoke opacity was carried out using the standard SAE J1667 snap-acceleration test. The engine was rapidly accelerated at full throttle for 4 s, and then returned to idle. The opacity was measured at full throttle, and the test was repeated twice.

2.4. Emission Analysis

The composition of the exhaust gas of the diesel car was analyzed using a FGA-4100A China Automotive Emission Analyzer, following the procedure described in [28]. The emission test was carried out by following the standard dual idle speed, as shown in Table 4.



Figure 2. Final setup for testing.

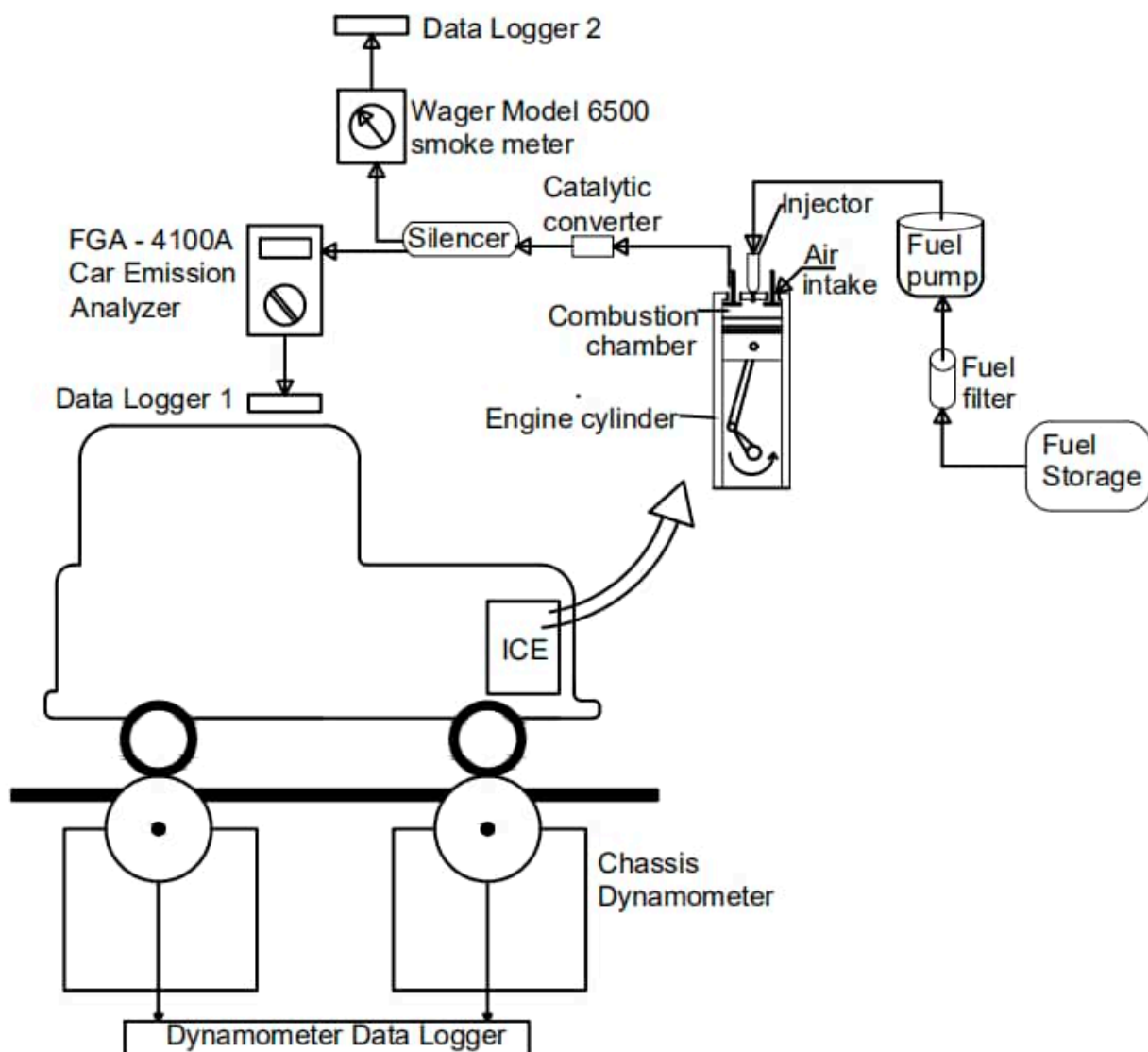


Figure 3. Schematic diagram of the experimental setup.

Table 4. Process of measuring exhaust ingredients.

	70% Rated Engine Speed		High Idle Speed			Low Idle Speed		
Time(s)	Hold	Wait	Hold	Read	Wait	Hold	Read	
	30	15	15	30	15	15	30	

2.5. Horsepower Test

The power and torque of the test car were measured using a computer-linked chassis dynamometer (dyno). To measure the wheel power and torque, the driving wheels of the test car were loaded on the rollers of the chassis dyno, as shown in Figure 4.

**Figure 4.** Vehicle exhaust removal system and rollers of the chassis dyno.

Calculation of horsepower by the chassis dynamometer:

$$P = \frac{2\pi\omega T}{60} \quad (1)$$

where P = power in kilowatts; T = torque in Newton meters; and ω = rotational velocity (rev/min).

2.6. Fuel Economy Test

The fuel economy test was conducted on a dyno based on full-load conditions at 650 rpm. The dyno measures the distance travelled by the car wheels after spending 50 mL of test fuel, as measured by the fuel measuring cup.

2.7. Optimization of Blend Ratio Using Artificial Methods

Extreme learning machine (ELM) is considered a new learning scheme for the single-hidden-layer neural network (SLFN) proposed by [29]. ELM randomly initializes the input weight and bias to get the corresponding output weight for an SLFN. Instead, these parameters are independent of the training data, due to their randomly assigned nature [30]. Then, the output weight is determined by the Moore–Penrose generalized inverse analysis, which is the connection between the hidden layer and the output layer [31]. Figure 5 below shows the structure of ELM.

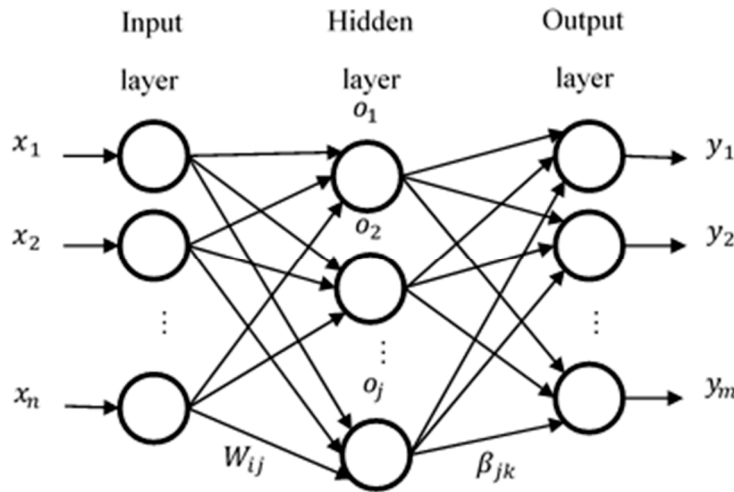


Figure 5. Structure of ELM.

For a training dataset D of N different training samples (X_i, t_i) , where $X_i = [x_{i1}, x_{i2}, \dots, x_{in}]^T \in R^n$ is the input vector and $t_i = [t_{i1}, t_{i2}, \dots, t_{im}]^m \in R^m$ is the target vector, the standard SLFNs with L nodes can be expressed as:

$$\sum_{i=1}^L \beta_i g_i(W_i \cdot X_j + b_i) = o_j \quad 1 \leq j \leq N \quad (2)$$

where $g(x)$ = activation function; $W_i = [w_{i,1}, w_{i,2}, \dots, w_{i,n}]^T$ is the weight vector connected with the i th hidden node and the input node; β_i = the weight vector connected with the output nodes; b_i = the threshold value of the i th hidden node; and $W_i \cdot X_j$ = the inner product of W_i and X_j . The hidden layer output matrix of the SLFN is calculated using:

$$H\beta = T \quad (3)$$

where H = the hidden layer output matrix of SLFN; β = the weight vector connected with the output node; and T = the expected output.

- Output weight

In the ELM algorithm, once the input weight W_i and the bias of the hidden layer b_i are randomly determined, the output matrix of the hidden layer H is uniquely determined. The training of the SLFNs can be transformed into solving a linear system. Hence, the output weight is determined by the matrix:

$$\beta = H^\dagger T \quad (4)$$

- Objective function

Since the model of the biodiesel engine is established with ELM, an objective function is defined to optimize the biodiesel ratio. In this study, the target functions are the fuel economy, emission standards, and power output of the engine. The objective function, f_{obj} , is therefore formulated using Equation (4):

$$\begin{aligned} f_{obj} = \min(w_{cost} & N(M_{cost}(x)) + w_{power}N(M_{power}(x)) \\ & + w_{smoke}N(M_{smoke}(x)) + w_{CO}N(M_{COhigh}(x)) \\ & + w_{CO}N(M_{COflow}(x)) + w_{NO_x}N(M_{NO_xhigh}(x)) \\ & + w_{NO_x}N(M_{NO_x}(x)) + w_{HC}N(M_{HChigh}(x)) \\ & + w_{HC}N(M_{HClow}(x)) = \min(fitness\ function) \end{aligned} \quad (5)$$

where $N(\cdot)$ = normalization function; x = input biodiesel ratio; $M_{cost}(x)$ = fuel economy; $M_{power}(x)$ = prediction model of maximum engine power; $M_{smoke}(x)$ = prediction model of smoke emission; $M_{COhigh}(x)$ = prediction model of CO emission at high idle speed; $M_{COLow}(x)$ = prediction model of CO emission at low idle speed; $M_{NOxhigh}(x)$ = prediction model of NO_x emission at high idle speed; $M_{NOxlow}(x)$ = prediction model of NO_x emission at low idle speed; $M_{HChigh}(x)$ = prediction model of HC emission at high idle speed; $M_{HClow}(x)$ = prediction model of HC emission at low idle speed; and $w_{power} \in [1, 3]$, $w_{cost} \in [1, 3]$, $w_{HC} \in [1, 3]$, $w_{CO} \in [1, 3]$, $w_{NOx} \in [1, 3]$ and $w_{smoke} \in [1, 3]$ are the user-defined weights corresponding to power, fuel economy, HC, CO, NO_x , and smoke, respectively.

- Normalization

The normalized function is used to convert the value of the objective component to the range $[0, 1]$, so as to ensure that each element contributes equally to the objective function. The weights of f_{obj} are defined according to the general requirements of in-use diesel vehicles. Table 5 shows user-defined weights for the objective function.

Table 5. Weights in the objective function.

Weight	Value
w_{cost}	1.5
w_{power}	1.0
w_{smoke}	3.0
w_{CO}	1.0
w_{NOx}	2.0
w_{HC}	1.0

3. Results

- Fuel properties

ASTM D6751 [32] specifies various test methods to be used in the determination of certain properties of biodiesel, such as flash point, kinematic viscosity, etc. The standard specifies a cetane number equal to or greater than 47 for biodiesel that could substitute for conventional diesel. The summary of the fuel properties determined by ASTM D6751/EN 14,214, as presented in Table 6, reveals that the grape seed FAME biodiesel meets the international standard of biodiesel. Although grape seed FAME is a renewable fuel, its heating value is lower than that of conventional diesel, but well above the minimum European biodiesel standards (35 MJ/kg). A major factor that affects the power output of biodiesel is its blend. Hence, for optimal emission and power performance under specific load conditions, it is recommended to blend the biodiesel in appropriate proportions with conventional diesel for use in CI-engine-powered vehicles.

Table 6. Summary of fuel properties.

Properties	Grape Seed FAME	Diesel
Viscosity at 25 °C (mm^2/s)	7.47	5.5–24
Cetane number	47	45–50
Heating value (J/g)	39,440.97	47,424.79

- Smoke opacity test

Figure 6 shows the variation in smoke opacity at various blending levels. The result of the smoke opacity test reveals that B100 produces the least carbon soot, while B0 is the worst. The smoke density of B100 is 95.3% lower than the smoke density of B0, which implies that the smoke density decreases with the increase in the proportion of GS FAME. This proves that combustion of grape seed FAME may cause less smoke from diesel engines.

Therefore, blending of grape seed FAME with diesel will be one of the solutions to the high smoke opacity of diesel engine emissions.

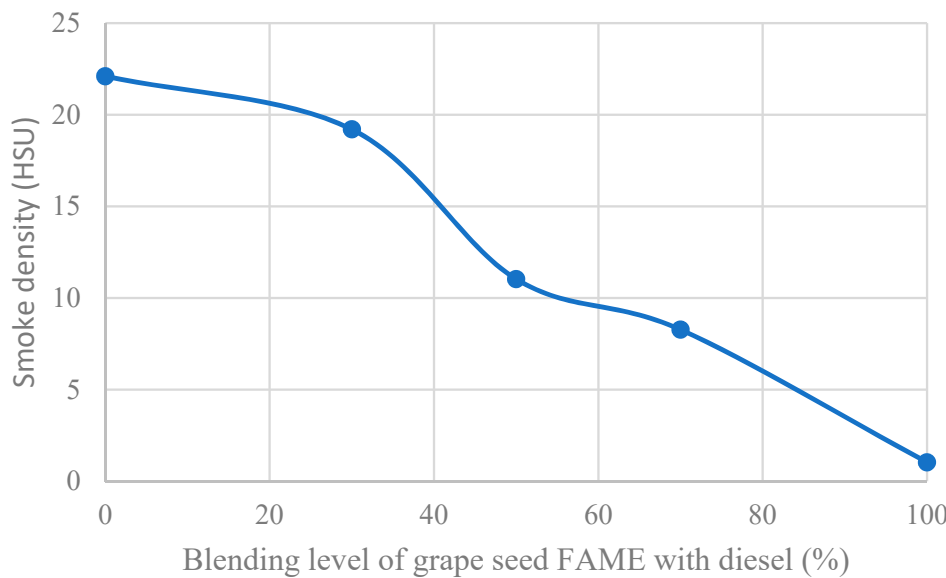


Figure 6. Variation in smoke opacity at various blending levels.

- HC emissions

Figure 7a,b show that the variation of HC emissions is a parabola. Increasing the proportion of GS biodiesel, there is an increase in HC emissions, which is supported by [33]. However, there is a noticeable decline in HC emissions as the proportion of GS biodiesel exceeds 50%. B100 has extremely low HC emissions at high idle speed and low idle speed compared to those of B0. Furthermore, B100 has no HC emissions at low idle speed. A blending level of 50% had the highest HC emissions compared to others. This result implies that the blending of conventional diesel and grape seed FAME in equal volumes or proportions may increase the HC emissions.

- CO emissions

CO emissions show great improvement for grape seed FAME compared with conventional diesel fuel at high idle speed, but not at low idle speed. From Figure 8a,b, the B30, B50, and B70 blends show no significant variation in CO emissions. The blends of grape seed FAME with diesel even performed worse compared with pure diesel and pure grape seed FAME. The reason for this phenomenon may be associated with the air–fuel ratio which is the ideal ratio of air to fuel that burns the fuel completely with no excess air [33]. A rich air–fuel mixture would have an incomplete combustion, thereby reducing the combustion efficiency. The vehicle may require more oxygen injection into the engine.

- NO_x emissions

NO_x emissions are of great concern in environmental pollution, leading to smog formation. From Figure 9a,b, B70 has the lowest value of NO_x emissions when compared to B0 and B100. It can also be observed that B50 shows high NO_x emissions and a high difference between maximum and minimum values, indicating the unstable performance of B50 in terms of NO_x emissions at high idle speed. This is supported by previous studies that have shown that NO_x emissions increase with pure biodiesels and their blends [14,18,34].

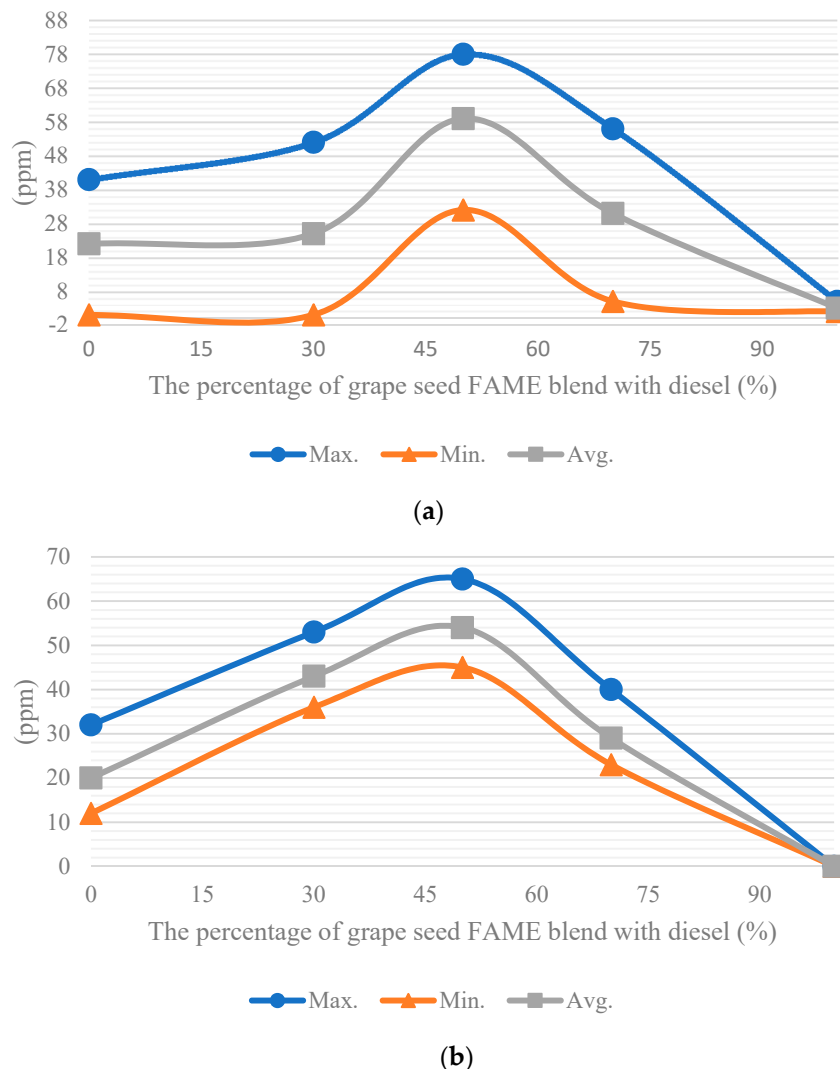


Figure 7. Graph of HC emissions against FAME blend at (a) high idle speed and (b) low idle speed.

- Exhaust gas temperature

From Figure 10a,b, the exhaust gas temperatures in the B0, B30, and B70 blends are extremely similar. B50 is much higher than other blending ratios, and also has the highest exhaust temperature. The exhaust temperature for B0 was the lowest.

- Horsepower

In Table 7, B0 gives the highest horsepower, followed by B100, while the lowest is from B30. It can be observed that the higher the ratio of GS FAME blended with diesel, the higher the horsepower. Furthermore, the horsepower of B100 is better than that of other blends.

Table 7. The data of different fuels tested with the chassis dynamometer.

Blend	Brake (rpm)	Speed (km/h)	Horsepower (kW)	Torque (Nm)
B0	331.79	20.65	5.33	153.38
B30	315.08	19.61	4.53	137.60
B50	335.34	20.88	4.74	134.96
B70	329.27	20.50	4.75	137.86
B100	325.47	20.26	4.84	142.08

- Fuel economy

Table 8 presents the results of the fuel economy test. The GS (70%)-DI (30%) blend (B70) performed the best, while the pure GS FAME (B100) had the worst fuel economy.

Table 8. Fuel economy test.

Blend	Fuel Economy (km/L)
B0	4.42
B30	4.02
B50	3.74
B70	5.41
B100	3.35

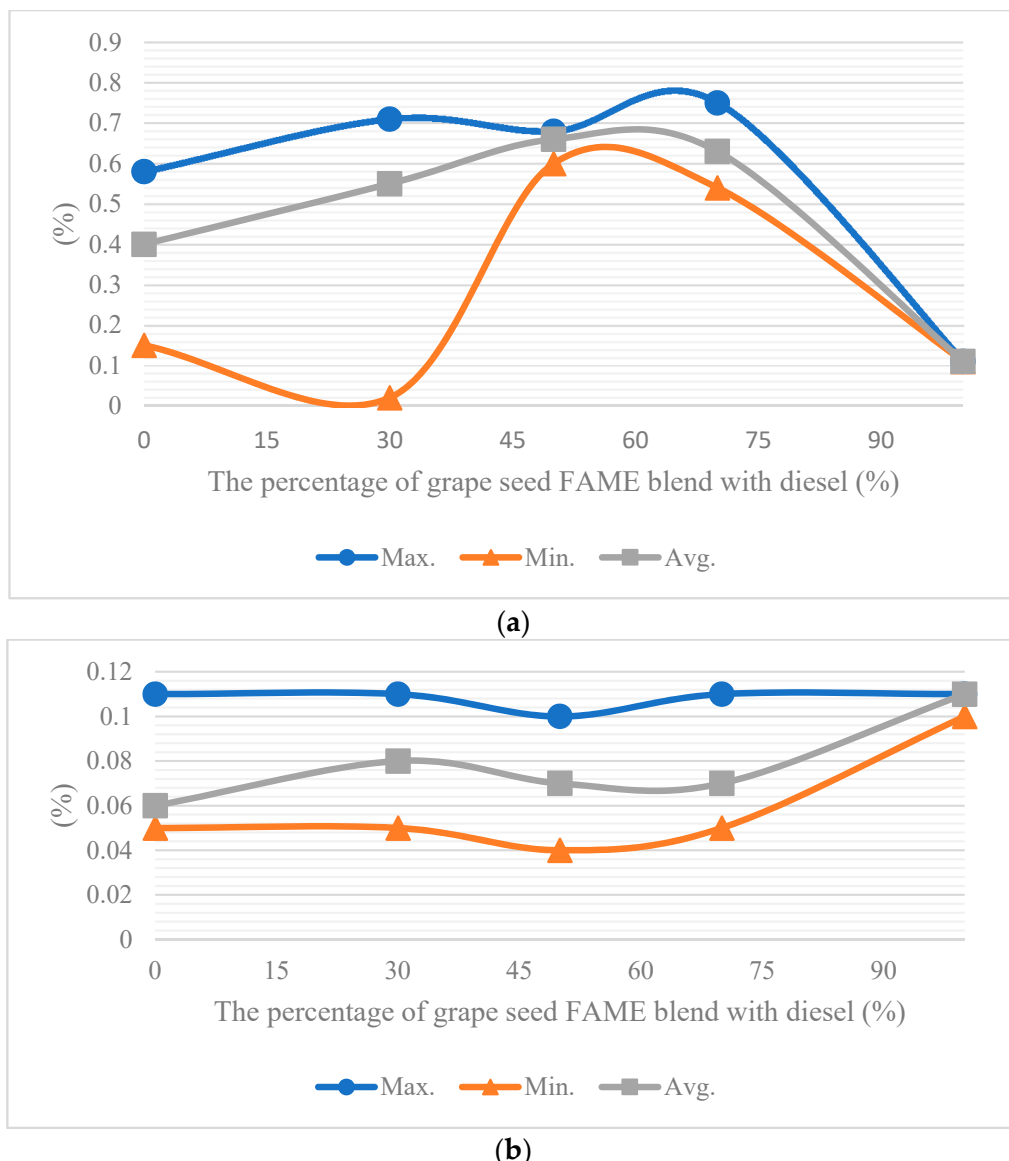


Figure 8. Graph of CO emissions against FAME blend at (a) high idle speed and (b) low idle speed.

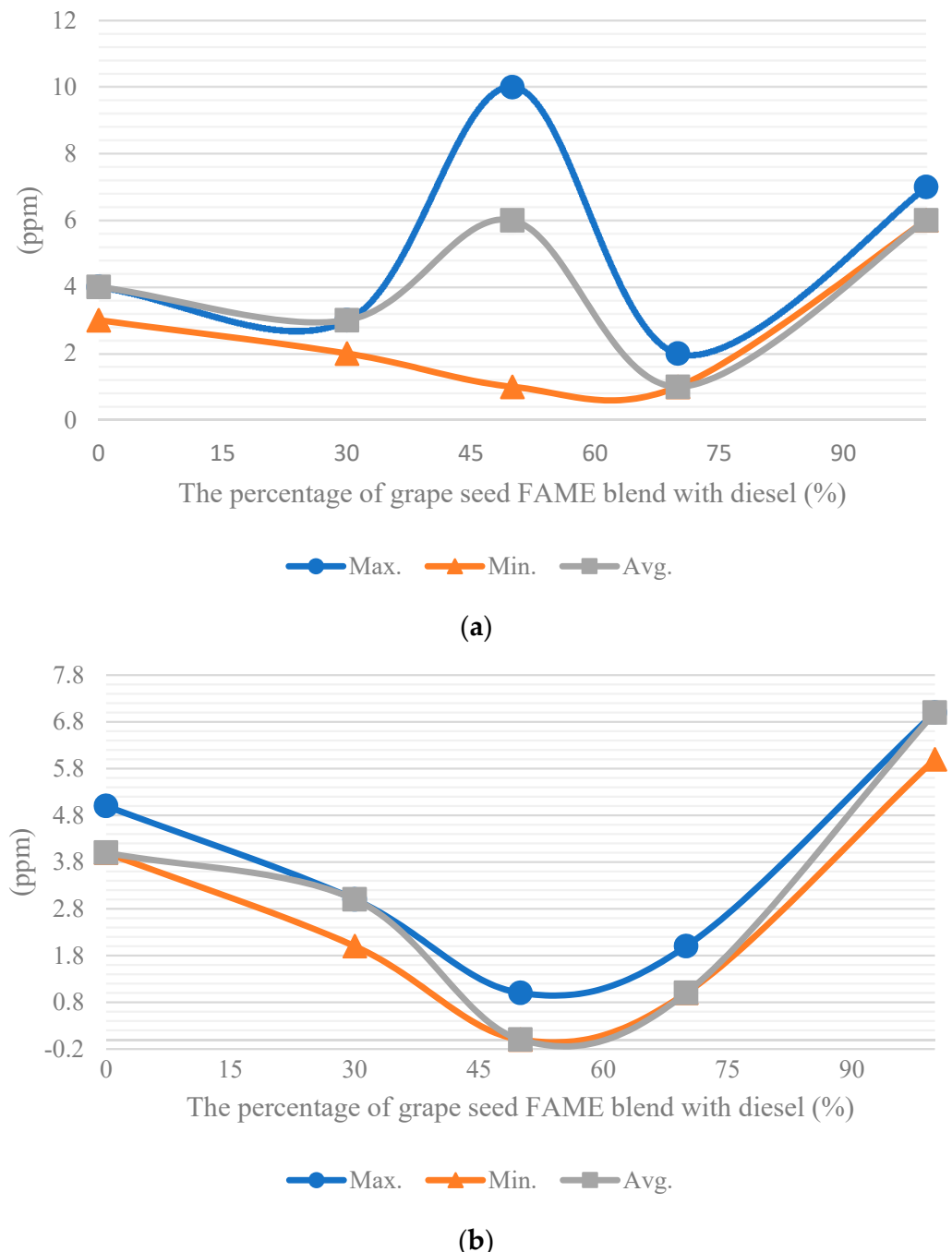


Figure 9. Graph of NO_x emissions against FAME blend at (a) high idle speed and (b) low idle speed.

- ELM Model Training and Testing

As the modelling technique is data-driven, sample experimental data are required to train the model. Table 9 summarizes the experimental data obtained from the combustion of different blends of grape seed FAME and conventional diesel in an internal combustion engine for the training of the ELM model. Since the data are dependent on the engine speed, they were collected based on standard dual idle speeds and standard engine test speeds in order to fairly evaluate the biodiesel engine performance.

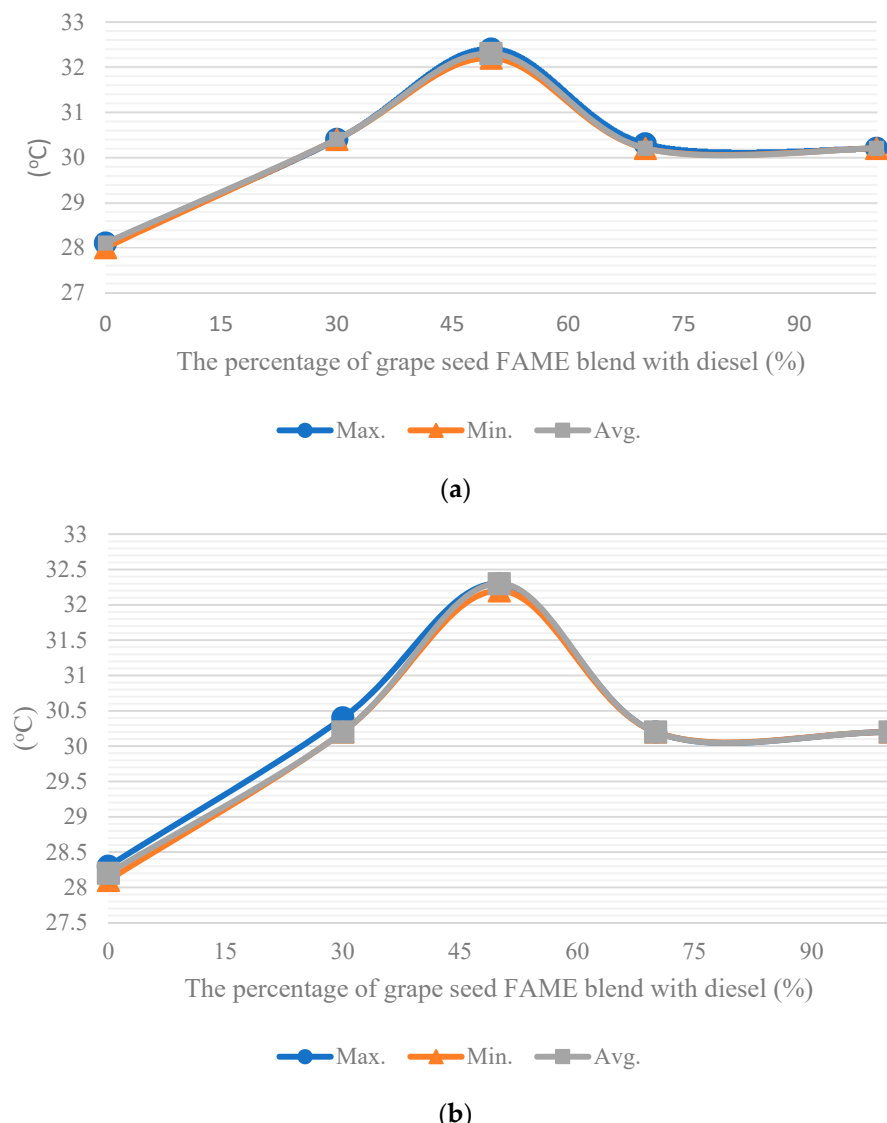


Figure 10. Graph of exhaust gas temperature against FAME blend at (a) high idle speed and (b) low idle speed.

Table 9. Training data.

	Dataset No., i	1	2	3	4	5
t_i	Biodiesel ratio (vol.%)	0	30	50	70	100
X_i	Maximum power at minimum engine speed (kW)	5.33	4.53	4.74	4.75	4.84
	Smoke opacity (HSU)	22.1	18	11.5	7.5	1.03
	HC at high idle speed (ppm)	22	25	59	31	3
	HC at low idle speed (ppm)	20	43	54	29	0
	CO at high idle speed (%)	0.4	0.55	0.66	0.63	0.11
	CO at low idle speed (%)	0.06	0.08	0.07	0.07	0.11
	NO_x at high idle speed (ppm)	4	3	6	1	6
	NO_x at low idle speed (ppm)	4	3	0	1	7
Fuel economy (km/L)		4.42	4.02	3.74	5.41	3.35

After the biodiesel engine model was built by the ELM and training data, each training datum was entered into the ELM model to calculate their accuracy one by one. The accuracy was measured by the percentage error. The average accuracy of the ELM model was found

to be $-1.2 \times 10^{-9}\%$, which is very low. Thus, the engine model shows enough accuracy for optimization. The percentage error was calculated using Equation (5):

$$E = \frac{(a - b)}{(b)} \times 100\% \quad (6)$$

where E = percentage error of the ELM model; a = training data; and b = predicted output data by the ELM model.

Table 10 below presents the results of accuracy test of ELM:

Table 10. Results of accuracy test.

Data Set No.	1	2	3	4	5	
Biodiesel ratio (vol.%)	0	30	50	70	100	Average of E for each index ($10^{-9}\%$)
Maximum power at minimum engine speed ($10^{-9}\%$)	-0.0066	-0.0066	0.2190	-0.0998	0.1100	0.0432
Smoke opacity ($10^{-9}\%$)	-0.3930	2.0800	-8.100	5.5500	-63.2000	-12.8126
HC at high idle speed ($10^{-9}\%$)	1.2800	-3.230	-0.281	0.4960	-52.7000	-10.8870
HC at low idle speed ($10^{-9}\%$)	-0.0400	0.5420	-4.960	4.0400	0.0268	-0.0782
CO at high idle speed ($10^{-9}\%$)	0.6910	-1.140	0.8940	1.5000	-7.4800	-1.1070
CO at low idle speed ($10^{-9}\%$)	-1.0300	2.5500	100.00	-0.0363	-0.1530	20.2661
NO_x at high idle speed ($10^{-9}\%$)	-0.468	1.3000	6.1800	-33.800	2.7600	-4.8056
NO_x at low idle speed ($10^{-9}\%$)	-1.0200	3.3200	-0.025	-20.100	4.2300	-2.7190
Fuel economy ($10^{-9}\%$)	0.749	-2.710	2.650	0.716	1.320	0.5450
Average of E of individual dataset ($10^{-9}\%$)	-0.0271	0.301	10.7	-4.64	-12.8	-1.2932

- Genetic Algorithm (GA) Optimization Results

In the GA optimization, the number of generations, population size, and termination tolerance on the fitness value were 1000, 30, and 10^{-20} , respectively. Other settings were set to default. The results of GA optimization after 20 independent runs are shown below in Table 11.

Table 11. Results of optimization.

Result No.	Ratio (%)	Fitness
1	73.66965627	-340.5590531
2	73.66733668	-340.5590531
3	73.67026635	-340.5590531
4	73.66891823	-340.5590531
5	73.66715099	-340.5590531
6	73.67054817	-340.559053
7	73.67025633	-340.5590531
8	73.67140711	-340.559053
9	73.66666093	-340.5590531
10	73.66868675	-340.5590531

Table 11. Cont.

Result No.	Ratio (%)	Fitness
11	73.66823657	-340.5590531
12	73.67123271	-340.559053
13	73.66857724	-340.5590531
14	73.66904511	-340.5590531
15	73.66702082	-340.5590531
16	73.66861278	-340.5590531
17	73.66787028	-340.5590531
18	73.66616498	-340.559053
19	73.66541996	-340.559053
20	73.66661274	-340.5590531
Average	73.66848405	-340.55905

4. Discussion

From the fitness calculated by the training data under the same weights presented in Table 12 below, it is observed that for the biodiesel ratio of 0%, the fitness is -272.179, which is the maximum. For the optimized biodiesel ratio of 73.67%, the minimum fitness of -340.559 is obtained. However, from Equation (5), the minimum fitness has the optimal solution. Hence, the optimal biodiesel ratio obtained is 73.67% by volume.

Table 12. Fitness of different biodiesel ratios.

Biodiesel Ratio (%)	0	30	50	70	73.76	100	Average
Fitness	-272.179	-320.565	-335.865	-339.545	-340.559	-331.180	-319.867

Table 13 also summarizes all of the parameters investigated; a smaller number means a better performance. B100 has the best performance in term of smoke opacity, HC emissions, and CO emissions, but the worst heating value, NO_x emissions, and fuel economy. B0 has the lowest exhaust gas temperature and the highest horsepower. In addition, B100 has the second lowest exhaust gas temperature.

Table 13. Ranking of tested biodiesel (ranking 1–7: 1—best, 7—worst).

Parameter	B0	B30	B50	B70	B100
Heating value	2	1	4	5	7
Smoke opacity	7	6	3	2	1
HC emissions	2	4	5	3	1
CO emissions	2	3	5	4	1
NO _x emissions	6	3	5	1	7
Exhaust gas temperature	1	4	7	3	2
Horsepower	1	7	5	4	3
Fuel economy	4	5	6	3	7

Table 14 depicts the indices of the tested biodiesel. These indices, obtained from Table 13, are categorized into three, namely:

Table 14. Indices of the tested biodiesel.

Parameter	B0	B30	B50	B70	B100
Emission	17	16	18	10	10
Energy transfer	4	12	16	12	12
Overall index	22	28	29	17	20

- Index of emission, which is the sum of the rankings of smoke opacity and HC, CO, and NO_x emissions;
- Index of energy transfer, which is the sum of the rankings of heating value, exhaust gas temperature, and horsepower;
- Overall index, which entails the sum of rankings of all emissions, horsepower, and fuel economy.

From Table 14, a lower overall index means a better performance. B70 also has the lowest emission index. A large heating value, low exhaust gas temperature, and high horsepower refer to a high energy transfer efficiency. Therefore, diesel has a high energy transfer efficiency. If the fuel economy, horsepower, and emissions are considered with some weights, a medium level of performance does not cause an obvious disadvantage. Thus, B70 (70% GS–30% DI) is the best choice of blend ratio, as it has the lowest overall index.

5. Conclusions

Owing to the performance of biodiesel produced from grape seed oil when tested using a four-cylinder, four-stroke compression ignition (diesel)-engine-powered vehicle, grape seed oil has been demonstrated to be a good potential biodiesel. The properties of the biodiesel and its blends with conventional diesel were investigated and tested on a diesel vehicle. The experimental results show that, among the various biodiesel blends tested, B70 (70% GS-30% DI) has the lowest NO_x emissions and medium levels of other emissions, and if horsepower, fuel economy, and emissions are considered with some weights, B70 remains the best choice. Furthermore, the results obtained from the ELM also confirm that the blend ratio B73.67 (73.67% GS-26.33 DI) has the best performance. We can conclude that the biodiesel from grape seed oil holds great potential, and can substitute for conventional diesel both in pure biodiesel form and in blends as fuel for diesel vehicles.

Author Contributions: Conceptualization, A.F. and W.F.I.; methodology, W.F.I.; investigation, A.F.; resources, W.F.I.; writing—original draft preparation, A.F.; writing—review and editing, W.F.I.; supervision, W.F.I.; funding acquisition, W.F.I. All authors have read and agreed to the published version of the manuscript.

Funding: This research was funded by the Science and Technology Development Fund from Macau SAR (FCDT) (0033/2019/AMJ).

Institutional Review Board Statement: Not Applicable.

Informed Consent Statement: Not Applicable.

Conflicts of Interest: The authors declare no conflict of interest.

References

1. Naik, S.; Goud, V.; Rout, P.; Dalai, A. Production of first and second generation biofuels: A comprehensive review. *Renew. Sustain. Energy Rev.* **2010**, *14*, 578–597. [[CrossRef](#)]
2. Aydogan, H.; Hirz, M.; Brunner, H. The use and future of biofuels. *Int. J. Soc. Sci.* **2014**, *3*, 12–21.
3. U.S. Energy Information Administration. *Short-Term Energy Outlook*, July 2021; U.S. Energy Information Administration: Washington, DC, USA, 2021.
4. Unpaprom, Y.; Tipnee, S.; Rameshprabu, R. Biodiesel from green alga *Scenedesmus acuminatus*. *Int. J. Sustain. Green Energy* **2015**, *4*, 1–6.
5. Ogunkunle, O.; Ahmed, N.A. A review of global current scenario of biodiesel adoption and combustion in vehicular diesel engines. *Energy Rep.* **2019**, *5*, 1560–1579. [[CrossRef](#)]
6. Baz, W.A.; Nawar, L.S.; Aly, M.M. Production of biofuel from sugarcane bagasse wastes using *Saccharomyces cerevisiae*. *J. Exp. Biol. Agric. Sci.* **2017**. [[CrossRef](#)]
7. Dworakowska, S.; Bednarz, S.; Bogdal, D. Production of Biodiesel from Rapeseed Oil. 1st World Sustainability Forum, 1–30 November 2011. Available online: www.wsforum.org (accessed on 6 July 2021).
8. Ge, J.C.; Yoon, S.K.; Choi, N.J. Using Canola Oil Biodiesel as an Alternative Fuel in Diesel Engines: A Review. *Appl. Sci.* **2011**, *7*, 881. [[CrossRef](#)]

9. Ashraful, A.M.; Masjuki, H.H.; Kalam, M.A.; Fattah, L.R.; Imtenan, S.; Shahir, S.A.; Mobarak, H.M. Production and comparison of fuel properties, engine performance and emission characteristics of biodiesel from non-edible vegetable oils: A review. *Energy Convers. Manag.* **2014**, *80*, 202–228. [[CrossRef](#)]
10. Pramanik, K. Properties and use of jatropha curcas oil and diesel fuel blends in compression ignition engine. *Renew. Energy* **2003**, *28*, 239–248. [[CrossRef](#)]
11. Fernández, C.; Solana, M.; Fiori, L.; Rodríguez, J.; Ramos, M.; Pérez, Á. From seeds to biodiesel: Extraction, esterification, transesterification and blending of Jatropha curcas oil. *Environ. Eng. Manag. J.* **2015**, *14*, 2855–2864.
12. Fernandez, C.M.; Ramos, M.J.; Perez, A.; Rodriguez, J.F. Production of biodiesel from winery waste: Extraction, refining and transesterification of grapeseed oil. *Bioresour. Technol.* **2010**, *101*, 7019–7024. [[CrossRef](#)]
13. Samo, M.; Luliano, M. Enzymatic production of Biodiesel from Grapeseed oil. *Chem. Eng. Trans.* **2020**, *80*, 301–306.
14. Sreedhar, C.; Prasad, B.D. Investigating on Use of Different Blends of White Grape Seed Biodiesel and Diesel on 4-Stroke Single Cylinder DI Diesel Engine. *Int. J. Eng. Res. Appl.* **2015**, *5*, 18–23.
15. Karthikeyan, S.; Prathima, A.; Elango, A. An Environmental Effect of Vitis vinifera (Grape Seed Oil) Biofuel Blends in Marine Engine. *Int. J. Mol. Sci.* **2015**, *44*, 1856.
16. Devan, P.K.; Mahalakshmi, N.V. A study of the performance, emission and combustion characteristics of a compression ignition engine using methyl ester of paradise oil–eucalyptus oil blends. *Appl. Energy* **2009**, *86*, 675–680. [[CrossRef](#)]
17. Anand, B.; Saravanan, C.; Srinivasan, C. Performance and exhaust emission of turpentine oil powered direct injection diesel engine. *Renew. Energy* **2010**, *35*, 1179–1184. [[CrossRef](#)]
18. Di, Y.; Cheung, C.; Huang, Z. Experimental investigation on regulated and unregulated emissions of a diesel engine fueled with ultra-low sulfur diesel fuel blended with biodiesel from waste cooking oil. *Sci. Total. Environ.* **2009**, *407*, 835–846. [[CrossRef](#)] [[PubMed](#)]
19. Kaisan, M.U.; Pam, G.Y.; Kulla, D.M.; Kehinde, A.J. Effects of Oil Extraction Methods on Bio-diesel Production from Wild Grape Seeds: A Case Study of Soxhlet Extraction and Mechanical Press Engine Driven Expeller Methods. *J. Altern. Energy Sources Technol.* **2014**, *6*.
20. Canaci, M.; Ozsezen, A.N.; Arcaklıoglu, E.; Erdil, A. Prediction of performance and exhaust emissions of a diesel engine fueled with biodiesel produced from waste frying palm oil. *Expert Sys. Appl.* **2009**, *36*, 9268–9280. [[CrossRef](#)]
21. Thirumurugan, M.; Sivakumar, V.M.; Merly Xavier, A.; Prabhakaran, D.; Kannadasan, T. Preparation of biodiesel from Sunflower oil by transesterification. *Int. J. Biochem. Bioinform.* **2012**, *2*, 441. [[CrossRef](#)]
22. Hoseinir, S.S.; Najafi, G.; Sadeghi, A. Chemical characterization of oil and biodiesel from Common Purslane (*Portulaca*) seed as novel weed plant feedstock. *Ind. Crop. Prod.* **2019**, *140*, 111582. [[CrossRef](#)]
23. Kamel, D.A.; Farag, H.A.; Amin, N.K.; Zatout, A.A.; Ali, R.M. Smart Utilization of Jatropha (*Jatropha curcas Linnaeus*) seeds for biodiesel production: Optimization and mechanism. *Ind. Crop. Prod.* **2018**, *111*, 407–413. [[CrossRef](#)]
24. Mironeasa, S.; Leahu, A.; Codina, G.; Stroe, S.; Mironeasa, C. Grapeseed: Physico-chemical, structural characteristics and oil content. *J. Agroaliment. Process. Technol.* **2010**, *16*, 1–6.
25. Fukuda, H.; Kondo, A.; Noda, H. Biodiesel fuel production by transesterification of oils. *J. Biosci. Bioeng.* **2001**, *92*, 405–416. [[CrossRef](#)]
26. Oliveira, L.S.; Franca, A.S.; Camargos, R.R.; Ferraz, V.P. Coffee oil as a potential feedstock for biodiesel production. *Bioresour. Technol.* **2008**, *99*, 3244–3250. [[CrossRef](#)]
27. Ramos, M.J.; Fernández, C.M.; Casas, A.; Rodríguez, L.; Pérez, Á. Influence of fatty acid composition of raw materials on biodiesel properties. *Bioresour. Technol.* **2009**, *100*, 261–268. [[CrossRef](#)]
28. Rondon, A.; Aliaga, R.; Cuisano, J. Fuel Consumption and Emissions Analysis of a Light Vehicle Fuelled with Two Ethanol-Gasoline Blends in Urban Driving Conditions of Lima Metropolitan. *World Electr. Veh. J.* **2021**, *12*, 99. [[CrossRef](#)]
29. Huang, G.B.; Zhu, Q.Y.; Siew, C.K. Extreme learning machine: Theory and applications. *Neurocomputing* **2006**, *70*, 489–501. [[CrossRef](#)]
30. Penrose, R. A generalized inverse for matrices. In *Proceedings of the Cambridge Philosophical Society*; Cambridge University Press: Cambridge, UK, 1955; pp. 406–413.
31. Huang, G.B.; Wang, D.H.; Lan, Y. Extreme learning machines: A survey. *Int. J. Mach. Learn. Cybern.* **2011**, *2*, 107–122. [[CrossRef](#)]
32. ASTM International. ASTM International. ASTM D6751-20a: Standard Specification for Biodiesel Fuel Blend Stock (B100) for Middle Distillate Fuels. In *Annual Book of ASTM Standards*; American Society of Testing Materials: West Conshohocken, PA, USA, 2020; Available online: www.astm.org (accessed on 7 June 2021).
33. Deng, B.; Li, Q.; Chen, Y.; Li, M.; Liu, A.; Ran, J.; Xu, Y.; Liu, X.; Fu, J.; Feng, R. The effect of air/fuel ratio on the CO and NO_x emissions for a twin-spark motorcycle gasoline engine under wide range of operating conditions. *Energy* **2018**, *169*, 1202–1213. [[CrossRef](#)]
34. Elango, T.; Senthilkumar, T. Performance and emission characteristics of CI engine fueled with non-edible vegetable oil and biodiesel blends. *J. Eng. Sci. Technol.* **2011**, *6*, 240–250.